Electronically Configurable Molecular-Based Logic Gates

C. P. Collier,[1]* E. W. Wong,[1]* M. Belohradský,[1] F. M. Raymo,[1]
J. F. Stoddart,[1] P. J. Kuekes,[2] R. S. Williams,[2] J. R. Heath[1]†

Logic gates were fabricated from an array of configurable switches, each consisting of a monolayer of redox-active rotaxanes sandwiched between metal electrodes. The switches were read by monitoring current flow at reducing voltages. In the "closed" state, current flow was dominated by resonant tunneling through the electronic states of the molecules. The switches were irreversibly opened by applying an oxidizing voltage across the device. Several devices were configured together to produce AND and OR logic gates. The high and low current levels of those gates were separated by factors of 15 and 30, respectively, which is a significant enhancement over that expected for wired-logic gates.

The fields of microelectronics and computation have advanced at an amazing rate over the past few decades, and at the heart of these advances has been the technology of the complementary metal-oxide semiconductor (CMOS)–based integrated circuit. However, both the fundamental physics of CMOS devices and the increasingly prohibitive costs associated with constructing next-generation fabrication facilities indicate that this technology is rapidly maturing. Nevertheless, the physics of computation is still in its infancy (1). Many researchers are exploring alternatives to CMOS-based computational machinery, including such options as single-electron transistors (2), quantum cellular automata (3, 4), molecular computation (5), and chemically assembled electronic nanocomputers (CAENs) (6). CAENs are proposed as extensions of conventional circuitry and architecture and will be based on chemically synthesized and assembled nano- or molecular-scale components. Very small machines containing vast amounts of resources (that is, moles of devices) may be possible, yet their basic operating and programming principles will be essentially the same as for present systems. However, there are many obstacles to the construction of an operational CAEN. For example, any chemically prepared system will be ordered (that is, crystalline) and defective (due to finite chemical reaction yields), whereas any reliable computational machine requires perfect complexity. Thus, any CAEN will have to be able to tolerate an extremely large number of defects.

Some of us recently reported on the Teramac CMOS-based supercomputer and commented on its relevance to an architecture for

a CAEN (7). Teramac was constructed from a very large number of partially defective resources and, as built, was not hard-wired as a computer at all. Instead, software routines were used to identify defective components and to subsequently download the logical architecture of a desired computer into a configuration memory that appropriately connected the usable hardware resources. Although there were several keys to the hardware architecture that made this possible, one of the primary lessons of Teramac for nanotechnology was that wires and configurable switches were likely to be the most plentiful and therefore important resources in a defect-tolerant CAEN. The configured logic elements of Teramac were "fine grained," meaning that the basic unit of control was the connection of two wires, not two large busses. Thus, to be economically viable, CAENs must be assembled from extremely inexpensive wires and configurable switches with simple techniques that are amenable to mass production.

Here we describe a first experimental step toward extending the architectural ideas of the Teramac computer to a CAEN. We have developed an electronically (singly) configurable junction that consists of a molecular monolayer and a tunneling barrier sandwiched between lithographically fabricated metal wires (Fig. 1). We demonstrate that this junction can be used as a switch, and that several devices, fabricated in a linear array structure, could be used as electronically configurable wired-logic gates (an AND and an OR gate). Because these switches are only singly configurable, they cannot be used for random access memory (RAM) applications, although programmable read only memory (PROM) applications are possible. However, they do have several advantages. First, and most importantly, they should scale down to molecular dimensions without appreciable loss of performance (8). Second, when the molecular switches are closed, current flows by resonant tunneling into the molecular electronic states. The net result of this resonant tunneling is that the high and low current levels of the logic gate truth tables are widely separated. This should lead to good noise immunity in future logic circuits built with this technology. Third, molecular switches are voltage addressable rather than field addressable. This makes the device robust with respect to dimensional tolerances in manufacturing. In a CMOS-based configurable device (9), two wires (address lines) are used to configure the switch, whereas two different wires (data lines) are used to read it. For our junctions, only two wires are necessary to achieve both functions. One voltage is applied to read the device, and a voltage of opposite polarity is applied to configure it. The configuration voltage of our devices can be a factor of 2 greater than the logic levels used when they are operating. This means that it should be easy to design circuits that are safe from accidental reconfiguration under operation conditions. Finally, this archi-
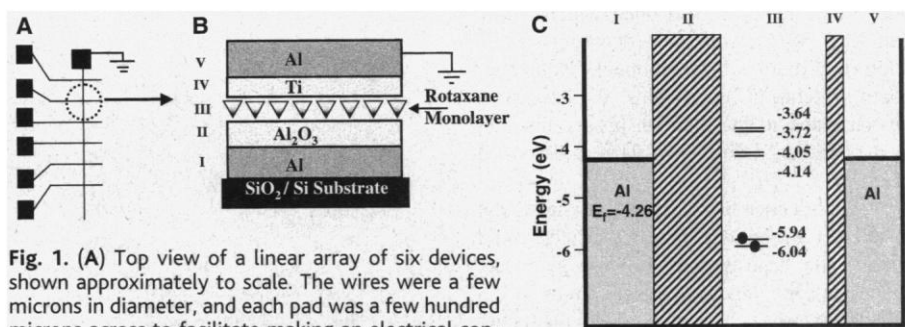

Fig. 1. (A) Top view of a linear array of six devices, shown approximately to scale. The wires were a few microns in diameter, and each pad was a few hundred microns across to facilitate making an electrical connection to the device. **(B)** Side view cross section of a single device junction. Each device consisted of a monolayer of molecules sandwiched between two perpendicularly oriented electrodes and contained several million molecules. **(C)** The energy level diagram of one of the devices in (A). The Fermi levels (E_f) of the Al electrodes are shown at both ends of the diagram, and discrete molecular redox energy levels [determined by solution-phase voltammetry measurements of the R(1) rotaxane] are shown in the middle. The oxidation states are noted with filled circles. The diagonally striped areas between the electrodes and the rotaxane energy levels are tunneling barriers. The thick barrier is the Al_2O_3 passivating layer (measured to be 1 to 1.5 nm), and the thin barrier is the Ti-rotaxane interface (estimated to be 0.5 nm).

[1]Department of Chemistry and Biochemistry, University of California, Los Angeles, CA 90095–1569, USA. [2]Hewlett-Packard Laboratories, Palo Alto, CA 94304–1392, USA.

*These authors contributed equally to this work.
†To whom correspondence should be addressed. E-mail: heath@chem.ucla.edu

tecture is highly modular. We report here on the properties of three different molecular switches incorporated into sandwich devices composed of various combinations of metallic wires.

Our devices are distinct from other electronically configurable two-terminal devices, such as ferromagnetic crosspoint memories (MagRAM) (10). In MagRAM devices, the high and low levels are typically separated by changes in the junction resistance of less than 50%. Although suitable for memory applications, such small changes are not suitable for computation.

Top and cross-sectional views of one of our devices, and its corresponding energy level diagram, are shown in Fig. 1. The switches were prepared by first lithographically patterning 6-μm-diameter Al wires onto a silica substrate. Second, a single monolayer of one of three different molecules was deposited as a Langmuir-Blodgett (LB) film over the entire substrate (11). Finally, a second set of 11-μm-diameter wires, consisting of a thin (5 nm) bottom layer of Ti followed by a thicker (0.1 μm) layer of Al, was evaporated through a contact shadow mask by using electron beam deposition. In each device batch, many linear arrays of junctions, combining to yield several hundred individual devices, were prepared. In >90% of the device fabrication runs, no defective devices were found.

The molecular compounds we used come from a class of molecules known as rotaxanes (12). Rotaxanes consist of two or more components mechanically interlocked with one another: One of the components is dumbbell-shaped, and the remaining components are rings that become trapped on the dumbbell component, encircling part of the dumbbell. In the class of rotaxanes used here, the dumbbell component contained two bipyridinium units and the encircling rings were bis-para-phenylene-34-crown-10. The molecular structure of one [R(1)] of the three systems we used is shown in Fig. 2. The other two compounds used were R(0), which was just the dumbbell component with no rings, and R(2), which contained two rings encircling the dumbbell component. Rotaxane-based switches (12) and gates (13) have been demonstrated in the solution phase, although their operation differs from what is described here.

A major concern was related to whether the monolayer of one of these molecules could survive the deposition of the top electrode. When the compounds are transferred as an LB film, the structures are oriented with the highly branched hydrophobic heads pointing away from the surface. This part of the compound apparently provides a buffer layer between the Ti-Al electrode and the centrally located bipyridinium rings, where oxidation or reduction takes place. The use of the Ti electrodes with molecular junctions does have literature precedent (14). Whether some reaction between the

molecules and the Ti occurs is difficult to know. Nevertheless, the redox properties of these molecular compounds, as measured in solution, do translate suprisingly well into solid-state device properties (8). We successfully used Cr-Al or Ti-Au electrodes in place of the Ti-Al electrode and observed only minor changes in the measured device properties. However, some electrode combinations, such as an Al top electrode without Ti, did destroy the switching properties of the junctions, and we only observed nonresonant tunneling behavior when we probed those devices.

All electrical measurements were carried out in air and at room temperature. The current-voltage (I-V) scans for an R(1)-based device are shown in Fig. 3A. R(0)- and R(2)-based devices behaved similarly, with a few subtle differences that will be discussed elsewhere. If molecular-mechanical motions were occurring in the R(1)- and R(2)-based devices, the electronic signatures of that motion were quite subtle and not obvious from our measurements. No such signatures are observed in the solution-phase electrochemistry of these particular molecules. All voltages were referenced to a grounded top electrode as defined in Fig. 1. When the device was initially probed (read) with a reducing (negative) voltage, the current increased sharply with increasing voltage, up to a few tenths of a nanoamp at –2 V. If the device was similarly probed a second time, the current fell slightly (~20%), but on subsequent measurements the response remained stable (15). The switch was irreversibly opened by applying an oxidizing voltage of +0.7 V or more (16). Once a switch was opened, its status could again be read by applying a negative voltage. For an open switch, the measured current at −2 V was a factor of 60 to 80 less than that for a closed switch.

Some insight into what is happening to the actual molecular junction can be gained by re-plotting the I-V scans as a normalized density-of-states (NDOS) (17) (Fig. 3B). When
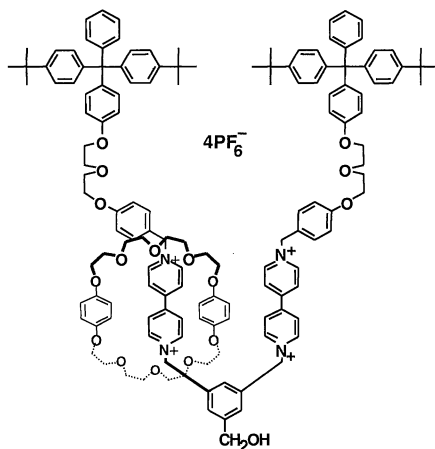

Fig. 2. A drawing of the R(1) rotaxane molecule used here.

the switch is shut, the NDOS at negative applied voltages is resolved into two features. The first broad peak can be understood in terms of the molecular redox states (Fig. 1B) derived from solution-phase pulsed voltammetry measurements. This feature corresponds reasonably well in energy to the lowest lying reduction features for solution-phase R(1), and is likely due to the same redox states. Thus, the onset of high current arises from resonant tunneling through these states. Tunneling mediated by molecular states has been observed previously in solution (18) and in solid-state devices (19). At voltages <−1.5 V, we believe that the device properties are not strongly correlated
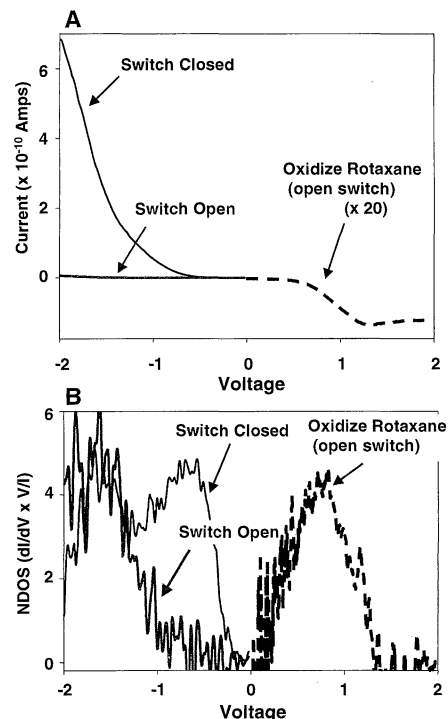

Fig. 3. (A) Current-voltage traces that show the operation of the devices. As prepared, the molecular switches are "closed," and the status of the devices is probed by applying a negative voltage to the bottom electrode. The switches are "opened" by oxidizing the molecules at voltages greater than +0.7 V. Finally, the open switches are again interrogated at negative bias. The current ratio at −2 V between open and closed states is between 50 and 70, depending on the specific device. (B) The same data as presented in (A), but plotted as the NDOS. When the closed switch is read, two distinct features are recorded in the NDOS. The first feature corresponds closely to the states shown in Fig. 1C. A single feature is observed in the oxidation NDOS. However, this feature is not a resolved electronic state. Rather, oxidation at around +0.7 to +0.9 V irreversibly changes the molecules, so the NDOS falls to 0 as the resonant tunneling process is quenched. When the oxidized devices are interrogated at negative voltage, the electronic states that were observed between 0 and 1 V for a "switch closed" device are now absent.

with the molecular electronic energy levels. We reach this conclusion because the simple linear amphiphile tunneling junctions we used as control devices exhibited similar behavior in this voltage range. After the device has been oxidized, the NDOS at negative biases between 0 and −1 V is essentially 0. The irreversible oxidation of similar molecules in solution has been previously documented [11] and is one reason that these compounds were used here. The fact that all three molecules exhibited similar behavior indicates that the dumbbell, rather than the crown ether rings, dominates the electronic properties of the junction. We successfully modeled both the *I-V* and the NDOS curves of Fig. 3 using the energy level diagram shown in Fig. 1C [8]. This calculation provided further evidence for the correspondence between the solution-phase and solid-state redox properties of these systems.

Several "control" devices were fabricated
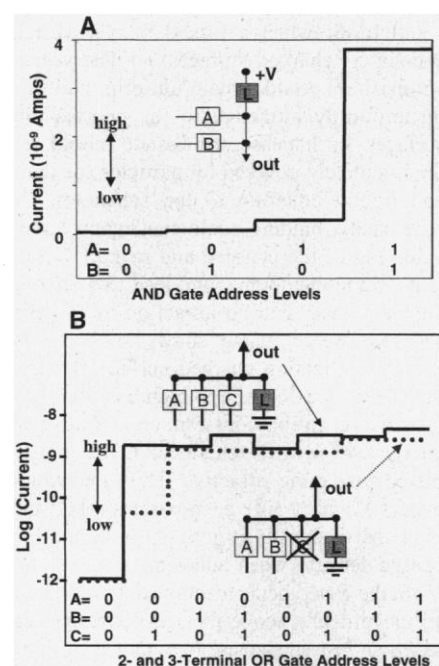
Fig. 4. Experimentally measured truth tables for logic gates configured from linear arrays of molecular switch junctions. For all logic gates, a low input is held at ground, and a high input is held at +2 V. Arbitrary high and low output current levels are assigned on each plot. The inputs are labeled alphabetically, and one device, labeled L, was configured as a load impedance on the gate. (**A**) The current output of a two-terminal AND gate as a function of input address, with an accompanying schematic of how the device was configured. (**B**) The current output (plotted on a logarithmic scale) for a three-input OR gate (solid trace), which was subsequently reconfigured into a two-input OR gate (dotted line) by oxidizing input C. For the two-input gate, the same truth table was measured, but input C was a dummy input. The [001] address state does raise the output current level, but not nearly enough to make the output "high."

in which LB monolayers of long-chain alkyl-carboxylate salts, such as $C_{19}H_{39}CO_2^-Na^+$, were used as the molecular layer. These linear amphiphiles acted as nonresonant tunneling barriers between the two electrodes, similar to what has been reported [20]. It was possible to increase the junction resistance of the control devices by oxidizing the Ti electrode at +2-V bias. However, because this process involved the diffusion of oxygen into the electrode, an initial oxidation step had a relatively small effect on the tunneling resistance. An extended (1-hour) oxidation at +2 V eventually led to a factor of 20 increase in tunneling resistance, as measured at −2 V. No measurable change in the NDOS of the junction was detected for the control devices, indicating that the control molecules themselves were not altered by the oxidation of the Ti electrode.

Once we had determined the conditions for addressing and configuring the individual devices, we were able to configure linear arrays of devices into AND and OR wired-logic gates. An experimentally derived truth table for a two-input AND gate is shown in Fig. 4A. On the scale of the y axis, experimental noise of the output current for a given input address state is not discernible. The truth table of any AND gate is such that a high response is only recorded when both inputs are high. Although the wired-AND gate presented here is simply a network of dissipative devices, its response is much better than would be expected from standard resistors. Even if one had complete flexibility in choosing the values for the resistors in a standard network, the maximum difference in current flow that one could hope for between the high and low states would be a factor of 2. However, we observed something closer to a factor of 15 because of the highly nonlinear *I-V* characteristics of our resonant-tunneling junctions. This nonlinearity is extremely useful because it should allow combination of wired-AND and wired-OR gates with each other to create more complex and intrinsically nonlinear logic circuits.

In Fig. 4B we present truth tables for an OR gate that was initially configured as a three-input OR gate, but then reconfigured as a two-input OR gate. The truth table of any OR gate is such that if any input combination is held high, then the output is high. For this experiment, the truth table of the three-input device was measured, and then the device corresponding to input C was oxidized. The same truth table was measured again, but with input C as a dummy variable. The point of this exercise was not only to demonstrate the reconfigurability of our devices, but also to investigate the issue of crosstalk between an operating gate and an interfering device somewhere else in the same circuit [21]. In this case, the interfering device was the oxi-

dized dummy input (labeled C in Fig. 4B) to the two-terminal gate. As seen from Fig. 4B, both versions of the OR gate yield quite high discrimination between low and high output states. The difference between high and low is at least a factor of 30, even for the reconfigured two-input gate.

These logic gates are similar in principle to diode-based wired-logic gates, with the exceptions that they are electronically configurable and that their behavior remains highly nonlinear over a broad voltage range. This means that the truth tables shown in Fig. 4 remain current-scaled versions of Fig. 4 at all operating voltages from −0.5 and −2.5 V, although they are substantially noisier at the lowest voltages. Furthermore, the simplicity of the fabrication process makes them inexpensive to produce. The simplicity of this device fabrication process makes it straightforward to quickly screen molecules for useful electronic properties. A clear target to screen for is a reconfigurable molecular switch, which would allow for the demonstration of random access memory as well as all logic functions [through the use of stored look-up tables [7]]. A second challenge will be to scale down the size of the device and integrate molecular switches with molecular-scale wires, such as metallic carbon nanotubes. The fact that the electronic properties of our compounds are very similar in both the solid-state devices and in a dilute solution suggests that these devices should scale down in size without significant change in operation. The devices presented here provide a compelling argument that molecular switch devices may play an important role in future computational technologies.

References and Notes
1. R. P. Feynman, *Lectures in Computation*, A. J. G. Hey and R. W. Allen, Eds. (Addison-Wesley, Menlo Park, CA, 1996).
2. R. H. Chen, A. N. Korotov, K. K. Likharev, *Appl. Phys. Lett.* **68**, 1954 (1996).
3. P. D. Tougaw and C. S. Lent, *J. Appl. Phys.* **75**, 181 (1994).
4. I. Amlani *et al.*, *Science* **284**, 289 (1999).
5. L. M. Adleman, *ibid.* **266**, 1021 (1994).
6. M. Montemerlo *et al.*, *Technologies and Designs for Electronic Nanocomputers* (MITRE Corporation, McLean, VA, 1996). Abstract available at http://www.mitre.org/resources/centers/wc3/nanotech/review_article.html
7. J. R. Heath, P. J. Kuekes, G. S. Snider, R. S. Williams, *Science* **280**, 1716 (1998).
8. We correlated the electrochemical properties of a dilute solution of these molecules with their electronic properties in these solid state devices. Thus, the device characteristics were determined by single-molecule properties. See the supplementary material available at www.sciencemag.org/feature/data/1039735.shl
9. Here we refer to a field programmable gate array (FPGA). A discussion of FPGAs and their applications to configurable computing can be found in J. Villasenor and W. Mangione-Smith, *Sci. Am.* **276**, 68 (June 1997).
10. W. J. Gallagher *et al.*, U.S. Patent 5 640 343 (1997).
11. LB films were transferred at: π = 28 mN/m and 59

Å²/molecule for R(0); π = 38 mN/m and 87 Å²/molecule for R(1); and π = 38 mN/m and 108 Å²/molecule for R(2). Previous work on LB films of similar molecules has been reported [D. B. Amabilino et al., New J. Chem. **1998**, 959 (1998)].

12. V. Balzani, M. Gomez-Lopez, J. F. Stoddart, Acc. Chem. Res. **31**, 405 (1998).
13. A. Credi, V. Balzani, S. J. Langford, J. F. Stoddart, J. Am. Chem. Soc. **119**, 2679 (1997).
14. C. Zhou, M. R. Deshpande, M. A. Reed, L. Jones II, J. M. Tour, Appl. Phys. Lett. **71**, 611 (1997).
15. These devices were operated under ambient conditions and no effort was made to exclude water or oxygen vapor. Their performance degraded over a period of a few days, similar to what would be expected for an unpackaged polymer-based electron-ic device. At voltages near ±3 V, the junction breaks down and an open circuit is measured. The overall device yield, based on measuring several hundred devices over ~20 separate fabrication runs, was greater than 95%.
16. We monitored the oxidation of the devices by holding the device at a positive (oxidizing) bias for extended periods, and then monitoring the current through the device at –2.0 V. Oxidation at +0.7 V took several minutes, but oxidation only took a few seconds at voltages above +1 V. When devices were oxidized at +0.5 V, the current flow at –2.0 V dropped only very slightly—by about 1% per minute of oxidation.
17. R. M. Feenstra, J. A. Stroscio, A. P. Fein, Surf. Sci. **181**, 295 (1987).
18. W. B. Davis, W. A. Svec, M. A. Ratner, M. R. Wasielewski, Nature **396**, 60 (1998).
19. K. W. Hipps and U. Mazur, J. Phys. Chem. **98**, 5824 (1994).
20. E. E. Polymeropoulos and J. Sagiv, J. Chem. Phys. **69**, 1836 (1978).
21. By the term "crosstalk," we are referring to complications that might arise when separate devices share a common electrode. One complication might be the unintentional oxidation of a device.
22. This work was supported by the Office of Naval Research (contract N00014-98-1-0422), the NSF-GOALI program, and Defense Advance Research Projects Agency.

2 March 1999; accepted 1 June 1999

Electrostatic Repulsion of Positively Charged Vesicles and Negatively Charged Objects

Helim Aranda-Espinoza,[1]* Yi Chen,[2] Nily Dan,[1]* T. C. Lubensky,[2] Philip Nelson,[2]† Laurence Ramos,[3] D. A. Weitz[2]‡

A positively charged, mixed bilayer vesicle in the presence of negatively charged surfaces (for example, colloidal particles) can spontaneously partition into an adhesion zone of definite area and another zone that repels additional negative objects. Although the membrane itself has nonnegative charge in the repulsive zone, negative counterions on the interior of the vesicle spontaneously aggregate there and present a net negative charge to the exterior. Beyond the fundamental result that oppositely charged objects can repel, this mechanism helps to explain recent experiments on surfactant vesicles.

Opposite charges attract in vacuum. Two ionizable objects in an electrolyte such as water form a more complex system, but nevertheless, in many situations a simple rule of thumb applies: As two planar surfaces approach from infinity, they initially attract if oppositely charged, with a screened Coulomb potential (1).

The analysis here was motivated by two sets of experimental observations that defy the familiar rule above (2, 3). Bilayer vesicles were prepared from a mixture of cationic (positively charged) and neutral surfactants. In one case, vesicles were allowed to adhere to a negatively charged substrate (2), while in the other, negatively charged colloidal particles were introduced into suspensions of vesicles and the resulting self-assembled struc-tures monitored (3). The puzzling observation was that despite the high charge on the vesicles, they were not uniformly attractive to the particles or surfaces, but instead separated macroscopically into adhesive and nonadhesive zones (Fig. 1). The vesicle diameter was typically 20 μm; the Debye screening length 1/κ was much smaller, between 1 and 10 nm (4). Because membranes in living cells also include bilayers made from mixtures of negatively charged and neutral lipids (5), phenomena like the ones reported here might occur generally.

The observed behavior is disturbingly counterintuitive and raises several questions: Why should adhesion to one zone of the membrane affect adhesion hundreds of screening lengths away? More urgently, why should electrostatic adhesion saturate in this way? How can oppositely charged objects repel?

The key to the puzzle is a subtle interplay between the entropic and electrostatic effects of the mobile counterions and laterally mobile lipids, which leads to a thermodynamic instability: The equilibrium state involves the coexistence of adhesive and repulsive zones in the membrane. The latter repel incoming negative objects by recruiting negative counterions on the interior face. The effects of demixing on membrane adhesion have been studied by other groups [for example, (2, 6)]. Our mechanism differs from earlier ones by including cooperative effects between counterions on both sides of an impermeable membrane. This effect can lead to adhesion saturation, a full discussion of which will appear elsewhere (7).

At least three possible equilibrium states could result when a mixed bilayer vesicle encounters charged surfaces: (i) The vesicle composition could remain uniform, and thus be uniformly attractive to the approaching surfaces. In this case, the vesicle should end up completely covered by particles (or tense and tightly adhering to the substrate). (ii) Alternately, binding could cause total lateral demixing of the charged and neutral surfactants in the membrane, and lead to a charge-depleted zone with no attraction to negative objects. One can easily show, however, that totally eliminating charged surfactants from the latter zone comes at a high cost in lateral distribution entropy; instead, enough residual charge will always remain to make the depleted zone quite attractive. Thus, one would expect at most (iii) a coexistence between high charge density (tight adhesion) and low charge density (weak adhesion) zones.

In the experiments mentioned, however, often none of the above three expectations was realized. Instead, adhesion saturated at some optimal coverage. Once this point was reached, the colloidal particles in (3) were not seen to leave or join the vesicle. Indeed, particles in suspension are seen to approach the vesicle, then bounce off. Similarly, the experiment in (2) found "blistering" in the contact region instead of uniform tight contact.

To confront this paradox, we begin with Parsegian and Gingell's classic analysis of the attraction of oppositely charged, planar surfaces (8). The authors studied the interaction of two infinite parallel planes with fixed bound surface charge densities $\sigma_+ > 0$ and $\sigma_- < 0$. Between the planes, a gap of width ℓ contains water, a dielectric medium with dielectric constant (9) $\epsilon = 80\epsilon_0$ with mobile point charges (ions) supplied by an external reservoir. We will consider all ions to be univalent, as in the experiment of (3). The

[1]Department of Chemical Engineering, University of Delaware, Newark, DE 19716, USA. [2]Department of Physics and Astronomy, University of Pennsylvania, Philadelphia, PA 19104 USA. [3]Groupe de Dynamique des Phases Condensées, Case 26, Université de Montpellier II, Place E. Bataillon, 34095 Montpellier Cedex 05, France.

*Address after 1 September 1999: Department of Chemical Engineering, Drexel University, Philadelphia, PA 19104, USA.
†To whom correspondence should be addressed.
‡Address after 1 September 1999: Department of Physics, Harvard University, Cambridge, MA 02138, USA.